ELSEVIER

Coordination Chemistry Reviews 224 (2002) 35–49

COORDINATION CHEMISTRY REVIEWS

www.elsevier.com/locate/ccr

Heteroselenometallic cluster compounds with tetraselenometalates

Qian-Feng Zhang [a], Wa-Hung Leung [b], Xinquan Xin [a,*]

[a] *Coordination Chemistry Institute and Department of Chemistry, Nanjing University, Nanjing 210093, People's Republic of China*
[b] *Department of Chemistry, The Hong Kong University of Science and Technology, Clear Water Bay, Kowloon, Hong Kong, People's Republic of China*

Received 17 November 2000; received in revised form 5 February 2001; accepted 26 March 2001

Contents

Abstract

The coordination cluster compounds of tetraselenomolybdate and tetraselenotungstate anions with metal ions are reviewed. New heteroselenometallic cluster compounds are primarily of interest regarding their structures and reactivities, and their potential as non-linear optical (NLO) materials. This article focuses from a synthetic and structural point of view on coordination cluster compounds with tetraseleno-molybdate and -tungstate anions as polydentate ligands. A comprehensive survey is presented of the heteroselenometallic clusters known to date according to the number of center $[MSe_4]^{2-}$ (M = Mo, W) anions. Representative spectroscopic and NLO properties of these clusters are also discussed.

Keywords: Molecular structures; Crystal structures; Heteroselenometalates; Selenide clusters; Tetraselenometalates; Spectroscopic data; Non-linear optical properties

1. Introduction

In the past two decades, the coordination chemistry of thiometalates has been extensively studied because this system is believed to be relevant to many important processes such as hydrodesulfurization (HDS) of crude oil [1], hydrogenation of unsaturated and aromatic hydrocarbons [2], and biosynthesis of metalloproteins [3]. Their rich structural chemistry has also received great attention and interesting investigation [4]. The chemistry of $[MO_nS_{4-n}]^{m-}$ (M = Re, $m = 1$; M = Mo and W, $m = 2$; M = V, $m = 3$; $n = 0$–2) is rich and

Abbreviations: acac, acetyacetonate anion $[CH_3C(O)CHC(O)CH_3]^-$; DMFN, *N*-dimethylformamide $HC(O)N(CH_3)_2$; DMSO, dimethylsulfoxide $(CH_3)_2SO$; dppe, 1,2-bis(diphenylphosphino)ethane $Ph_2PCH_2CH_2PPh_2$; dppm, 1,1-bis(diphenylphosphino)methane $Ph_2PCH_2PPh_2$; Et_4N^+, tetraethylammonium cation; NLO, non-linear optical; $PhMe_2P$, dimethylphenylphosphine; Ph_3P, triphenylphosphine; Ph_4P^+, tertaphenylphosphonium cation; py, pyridine C_5H_5N; THF, tetrahydrofuran C_4H_8O.

* Corresponding author. Tel.: +86-25-3593132; fax: +86-25-3314502.
E-mail address: xxin@netra.nju.edu.cn (X. Xin).

0010-8545/02/$ - see front matter
PII: S0010-8545(01)00371-X

diverse [5–8]. However, until ca. 1990 [9], the chemistry of selenometalates failed to keep abreast with that of the corresponding thiometalates, as witnessed by the sporadic reports of tetraselenometalates such as $[MoSe_4]^{2-}$ and $[WSe_4]^{2-}$. The delayed development of the chemistry of selenometalates is attributable to the following reasons. First, the most convenient method for synthesizing thiometallic anions involved the use of H_2S, and this was found to be unattractive for selenometallic anions because of the extreme toxicity of H_2Se. Second, an initial perception that the thiometalate and selenometalate systems are more or less chemically and structurally similar hindered research enthusiasm in the selenometallic area. As a result, much of our understanding of tetraselenometallic anion chemistry up to 1992 had been derived from the tetrathiometalate system [10].

There has been a facile method for synthesis of the tetraselenometallic anions $[MSe_4]^{2-}$ (M = Mo, W) which were prepared in satisfactory yield simply from the oxidative reaction of polyselenide Se_x^{2-} ($x = 2$–4) with $M(CO)_6$ in DMF solution [11]. Müller et al. first reported a classic cubane-like cluster compound $[OMoSe_3Cl(CuPPh_3)_3]$ [12]. Afterwards, Ibers and coworkers synthesized a series of coinage-metal/$[WSe_4]^{2-}$ cluster compounds with linear, cubane and planar skeletons, in which the $[WSe_4]^{2-}$ anion was shown to act as a versatile ligand coordinating to one to four coinage-metal atoms [10,13–16]. Three review articles partly summarizing the structural chemistry of heteroselenometallic clusters have already appeared [8,17,18]. Since then, investigations have been made on the syntheses and structures of polynuclear and polymeric heteroselenometalates [19,20]. Our research in heteroselenometalate chemistry has been driven by the motivation to expand our knowledge of the reactivities and structures of tetraselenometallic ligands. Although there is a similarity between thiometalates and selenometalates with respect to reactivity and structure, the impetus in the study of selenometalate chemistry centers on the semiconducting and photoconducting properties, for which detailed structural characterization of the molecular forms is required [21]. Based on our knowledge of heterothiometallic clusters, especially their third-order non-linear optical properties [22], the research interest in the heteroselenometallic clusters has shifted from purely structural investigations towards the study of the structure–property relationship for NLO properties of metal clusters.

This review describes the preparations, structural and spectroscopic characterizations of heterometallic clusters with tetraselenometallic anions $[MSe_4]^{2-}$ (M = Mo, W) as well as the NLO properties of these clusters. The emphasis is on recent progress in this area of research; however, older literature is also cited when appropriate.

2. Survey of syntheses and structures of heteroselenometalates

2.1. Mono-Mo(W) center cluster compounds

The binuclear cluster compounds $[(MSe_4)(M'X)]$ with a M:M′ (M = Mo, W; M′ = Cu or Au) ratio of 1:1 were isolated from the reaction between equal molar amounts of $[MSe_4]^{2-}$ anions and metal complexes M′L (L = CN^-, SCN^- and Cl^-) in CH_3CN solution [14,16]. The strong σ donor ligand Me_2PhP can substitute CN^- anion to coordinate metal atoms. With excess Me_2PhP, trinuclear cluster compounds $[Ph_4P]_2[(CN)Cu(\mu\text{-}Se)_2M(\mu\text{-}Se)_2Cu(CN)]$ decompose to give binuclear cluster compounds $[Ph_4P]_2[(CN)Cu(\mu\text{-}Se)_2MSe_2]$ and a small complex specie $(Me_2PhP)_3Cu(CN)$ [14]. An unsuccessful attempt to fashion a trimetallic heteroselonometalate containing three different metal centers resulted in the formation of a monoanionic heteroselenometallic cluster $[Ph_4P][(Me_2PhP)_2Cu(\mu\text{-}Se)_2MoSe_2]$ [16]. There are no monoanionic heterosulfidometalates derived from the $[MS_4]^{2-}$ moiety (Eqs. (1) and (2)).

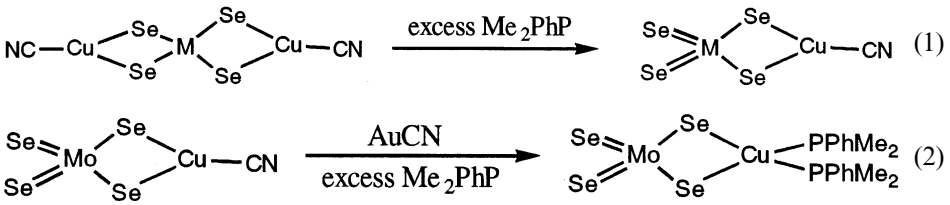

The coordination coinage-metal atoms show two types of trigonal and tetrahedral coordination, as illustrated in Fig. 1. The Mo–Se_t (t = terminal) bond distance in binuclear cluster compounds is similar to that in the $[MoSe_4]^{2-}$ anion (2.293(1) Å). The Mo–Cu distance of 2.857(1) Å in $[(Me_2PhP)_2Cu(\mu\text{-}Se)_2$-

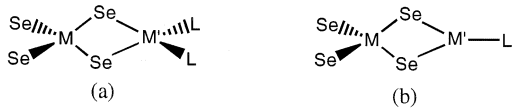

Fig. 1. Two structural sketches of bimetallic clusters with $[MSe_4]^{2-}$ (M = Mo or W; M′ = Cu or Au; L = ligands).

Table 1
Comparison of selected bond parameters of heteroselenometallic clusters

Compound	Mo(W)–Se (Å)	Mo(W)–Cu (Å)	Angle at Mo/W (°)	Reference
Cupro-selenometalates				
$[PPh_4]_2[Se_2Mo(\mu\text{-}Se)_2Cu(CN)]$	2.288(1)–2.368(1)	2.674(1)	108.39(5)–111.39(5)	[14]
$[PPh_4]_2[Se_2Mo(\mu\text{-}Se)_2Cu(PMe_2Ph)_2]$	2.294(1)–2.355(1)	2.857(1)	108.25(3)–110.19(3)	[16]
$[PPh_4]_2[(NC)Cu(\mu\text{-}Se)_2Mo(\mu\text{-}Se)_2Cu(CN)]$	2.331(1)–2.346(1)	2.684(1)–2.685(1)	108.93(3)–110.44(3)	[14]
$(\mu\text{-}WSe_4)[(PMe_2Ph)_2Cu]_2$	2.317(1)–2.327(1)	2.868(1)–2.877(2)	108.85(5)–110.01(3)	[10]
$[NEt_4]_2[\mu\text{-}WSe_4][(SC_4H_3)SeCu]_2$	2.338(1)–2.344(1)	2.699(2)	109.14(6)–109.97(4)	[13]
$(\mu_3\text{-}Cl)(\mu_3\text{-}MoSe_4)[(PPh_3)Cu]_3$	2.184(6)–2.388(4)	2.736(5)–2.768(5)	108.2(1)–112.0(3)	[30a]
$(\mu_3\text{-}Br)(\mu_3\text{-}MoSe_4)[(PPh_3)Cu]_3$	2.262(1)–2.383(1)	2.757(1)	108.4(1)–110.6(1)	[47]
$(\mu_3\text{-}I)(\mu_3\text{-}MoOSe_3)[(PPh_3)Cu]_3$	2.384(3)–2.385(4)	2.769(3)–2.795(4)	107.3(1)–112.4(6)	[32]
$(\mu_3\text{-}Cl)(\mu_3\text{-}WSe_4)[(PPh_3)Cu]_3$	2.201(4)–2.394(3)	2.733(3)–2.771(3)	108.13(8)–111.4(1)	[10]
$[PPh_4]_2[(\mu_3\text{-}MoOSe_3)(CuCl)_3py]$	2.391(1)–2.400(1)	2.667(2)–2.757(2)	109.18(5)–109.67(6)	[33]
$[NEt_4]_2[(\mu_3\text{-}MoSe_4)(Et_2NCS_2Cu)_3]$	2.317(2)–2.373(2)	2.724(2)–2.739(2)	108.4(1)–110.4(1)	[19]
$[NEt_4]_2[(\mu_3\text{-}WSe_4)(Et_2NCS_2Cu)_3]$	2.316(2)–2.373(2)	2.731(2)–2.747(2)	108.16(7)–110.05(7)	[34]
$[NEt_4]_2[(\mu_4\text{-}MoSe_4)(Me_2NCS_2Cu)_4]$	2.362(2)–2.371(2)	2.717(2)–2.731(2)	107.1(1)–110.4(1)	[19]
$[NEt_4]_2[(\mu_4\text{-}WSe_4)(Me_2NCS_2Cu)_4]$	2.337(2)–2.349(2)	2.693(2)–2.710(2)	106.34(7)–110.88(6)	[34]
$[(\mu_4\text{-}MoSe_4)Cu_4py_6Cl_2]$	2.360(2)–2.371(2)	2.712(1)–2.755(1)	107.9(1)–110.1(1)	[36]
$[(\mu_4\text{-}WSe_4)\{Cu(dppm)\}_4][ClO_4]_2$	2.3206(7)	2.8172(8)	108.12(4)–111.40(2)	[37]
$[Et_4N]_4[(\mu_6\text{-}MoSe_4)Cu_{10}(\mu\text{-}SPh)_{12}]$	2.378(2)	2.844(3)–2.886(2)	109.1(1)–110.2(1)	[19]
$[Et_4N]_4[(\mu_3\text{-}WSe_4)_3(Cu_3)_2(\mu_3\text{-}Se)_2]$	2.289(2)–2.400(2)	2.734(3)–2.741(2)	109.3(1)–110.2(1)	[31]
$\{[Et_4N]_2[(\mu_4\text{-}WSe_4)Cu_4(CN)_4]\}_n$	2.3382(10)	2.850(2)–2.907(2)	108.80(5)–109.68(5)	[20]
Argento-selenometalates				
$(PPh_3)Ag(\mu\text{-}Se)_2W(\mu\text{-}Se)_2Ag(PPh_3)_2$	2.320(1)–2.345(2)	2.9120(12)–3.0797(12)	106.99(7)–113.36(6)	[26b]
$(\mu\text{-}C_5H_5NS)(\mu\text{-}WSe_4)[(PPh_3)Ag]_2$	2.264(3)–2.398(3)	3.011(2)–3.017(2)	106.9(1)–113.98(8)	[27]
$(\mu_3\text{-}Cl)(\mu_3\text{-}MoSe_4)[(PPh_3)Ag]_3$	2.247(2)–2.374(2)	2.991(2)–2.979(2)	107.0(2)–111.96(9)	[30b]
$(\mu_3\text{-}Br)(\mu_3\text{-}WSe_4)[(PPh_3)Ag]_3$	2.221(4)–2.384(3)	2.984(3)	107.3(1)–111.6(1)	[30c]
$(\mu_3\text{-}I)(\mu_3\text{-}MoSe_4)[(PPh_3)Ag]_3$	2.237(2)–2.384(2)	2.994(1)–3.026(2)	107.4(3)–111.5(2)	[28]
$(\mu_3\text{-}I)(\mu_3\text{-}WSe_4)[(PPh_3)Ag]_3$	2.255(3)–2.372(4)	2.998(3)–3.079(2)	107.3(3)–111.8(3)	[28]
$(\mu_3\text{-}I)(\mu_3\text{-}WSe_4)[(Me_2PhP)Ag]_3$	2.262(1)–2.384(1)	2.976(1)	106.93(2)–111.89(2)	[15]
$\{[La(Me_2SO)_8][(\mu\text{-}WSe_4)_3Ag_3]\}_n$	2.2732(17)–2.3758(12)	2.9737(13)–3.0266(11)	106.43(6)–114.16(5)	[20]
Auro-selenometalates				
$[PPh_4]_2[Se_2Mo(\mu\text{-}Se)_2Au(CN)]$	2.281(2)–2.367(2)	2.795(4)	108.32(9)–112.7(1)	[16]
$[PPh_4][Se_2Mo(\mu\text{-}Se)_2Au(Me_2PhP)]$	2.278(1)–2.381(1)	2.852(1)	108.16(5)–112.38(5)	[16]
$[PPh_4][Se_2W(\mu\text{-}Se)_2Au(Me_2PhP)]$	2.283(1)–2.378(1)	2.872(1)	108.19(3)–112.14(3)	[16]
$(\mu\text{-}MoSe_4)[(PPh_3)Au]_2$	2.335(1)–2.351(1)	2.812(1)–2.819(1)	107.03(4)–113.59(4)	[25]
$(\mu\text{-}WSe_4)[(PMe_2Ph)Au]_2$	2.332(8)–2.350(6)	2.854(3)–2.858(3)	105.7(2)–112.8(2)	[10]
$(PPh_3)Au(\mu\text{-}Se)_2W(\mu\text{-}Se)_2Au(PPh_3)_2$	2.353(2)–2.362(2)	2.8642(12)–2.8893(13)	107.42(8)–113.06(7)	[12]
$(\mu\text{-}WSe_4)[(PPh_3)Au]_2$	2.318(10)–2.356(10)	2.854(5)–3.138(5)	107.1(4)–113.3(4)	[26b]
Other metal-selenometalates				
$[PPh_4]_2[(Se_2)Ni(\mu\text{-}Se)_2WSe_2]$	2.281(1)–2.357(1)	2.703(1)	106.44(3)–111.23(6)	[23]
$[PPh_4]_2[Se_2W(\mu\text{-}Se)_2Ni(\mu\text{-}Se)_2WSe_2]$	2.285(1)–2.350(1)	2.866(1)	103.62(3)–111.22(3)	[23]
$[MoFe_3Se_4(Et_2NCS_2)_6]$	2.364(2)–2.401(2)	2.741(2)–3.024(2)	107.9(1)–109.0(1)	[44]
$[NEt_4]_3[Mo_2Fe_6Se_8(SEt)_9]$	2.479(1)	2.793(2)	104.1(1)	[42]
$[NEt_4]_3[Mo_2Fe_7Se_8(SEt)_6(SC_6H_4Cl)_6]$	2.481(1)–2.499(1)	2.747(2)–3.316(1)	103.2(1)–105.4(1)	[42]
$[PPh_4]_4[Pb_2(WSe_4)_4]$	2.283(1)–2.352(1)	3.679(1)–3.872(1)	105.12(4)–112.41(5)	[45]
$[(\mu_3\text{-}WSe_4)_2(Pd_2)_2(\mu\text{-}dppm)_2]$	2.2699(14)–2.4149(10)	2.9382(8)–2.9496(8)	107.71(14)–110.66(15)	[40]

$MoSe_2]^{2-}$ is long compared with those in other Mo/Cu/Se binuclear clusters, and is slightly longer than the Mo–Au separations in Mo/Au/Se clusters [16]. Categorized according to coordination geometry/number/mode and the kind of coordinated metal atom, selected structural data of heteroselenometallic clusters are collected in Table 1.

The reaction of $Ni(acac)_2$ with $[NH_4]_2[WSe_4]$ in the presence of $[Ph_4P]\cdot Cl$ produced a binuclear W/Ni cluster compound $[Ph_4P]_2[Se_2W(\mu\text{-}Se)_2Ni(Se_2)]$ [23]. The only source of Se_2^{2-} in the dianion for this reaction is from the decomposition of the $[WSe_4]^{2-}$ anion. Very few examples for the formation of Se_2^{2-} from decomposition of the $[WSe_4]^{2-}$ anion have been reported. The structure of the $[Se_2W(\mu\text{-}Se)_2Ni(Se_2)]^{2-}$ anion (Fig. 2) is unique, having no sulfur analog in the literature. The

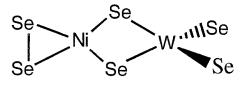

Fig. 2. The structural sketch of the $[Se_2W(\mu\text{-}Se)_2Ni(Se_2)]^{2-}$ anion.

Se–Se bond distance is 2.328(1) Å. The W atom center has a tetrahedral coordination geometry, while the geometry about the Ni atom is highly distorted square-planar.

The trinuclear cluster compounds $[Ph_4P]_2[(CN)M'(\mu\text{-}Se)_2M(\mu\text{-}Se)_2M'(CN)]$ (M = Mo, W; M′ = Cu, Au) were prepared by reacting $[Ph_4P]_2[MSe_4]$ with 2 equiv. of M′CN in CH_3CN solution [14]. In the presence of ligand Me_2PhP, this reaction led to replacement of CN^- groups to afford neutral clusters $[(Me_2PhP)Au(\mu\text{-}Se)_2M(\mu\text{-}Se)_2Au(Me_2PhP)]$, in which the Au atoms keep the trigonal coordination, and $[(Me_2PhP)_2Cu(\mu\text{-}Se)_2M(\mu\text{-}Se)_2Cu(Me_2PhP)_2]$, in which the Cu atoms have tetrahedral coordination [10]. Under similar reaction conditions, for the reaction of $Ag(PPh_3)Cl$ or $Au(PPh_3)Cl$ with $[Ph_4P]_2[MSe_4]$, the $[MSe_4]^{2-}$ anions simply link the two univalent units $[Ag(PPh_3)]^+$ and $[Au(PPh_3)]^+$ to give rise to clusters $[(PPh_3)Ag(\mu\text{-}Se)_2W(\mu\text{-}Se)_2Ag(PPh_3)]$ [24] and $[(PPh_3)Au(\mu\text{-}Se)_2Mo(\mu\text{-}Se)_2Au(PPh_3)]$ [25], respectively. Using $Ag(PPh_3)_2(NO_3)$ in place of $Ag(PPh_3)Cl$, $[(PPh_3)Ag(\mu\text{-}Se)_2W(\mu\text{-}Se)_2\text{-}Ag(PPh_3)_2]$, in which one Ag atom is trigonally coordinated and the other is tetrahedrally coordinated, was obtained [26]. Thus, the linear trinuclear clusters can be further classified into three types according to the coordination geometry of the coinage-metal atoms, as shown in Fig. 3.

On addition of excess C_5H_5NS to a CH_2Cl_2 solution of $[(PPh_3)Ag(\mu\text{-}Se)_2W(\mu\text{-}Se)_2Ag(PPh_3)_2]$, C_5H_5NS attaches to the framework, one PPh_3 ligand is detached, resulting in the formation of an incomplete cubane cluster $[(\mu\text{-}WSe_4)(AgPPh_3)_2(\mu\text{-}C_5H_5NS)]$ [27]. Thus, the linear structure can be converted to a butterfly configuration (Eq. (3)).

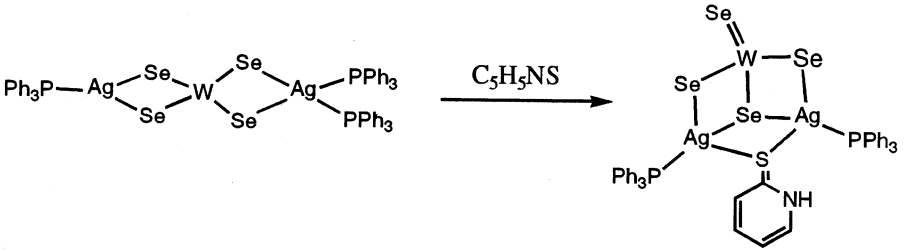

(3)

In the reaction of $[Et_4N]_2[WSe_4]$ and $Li[(CN)Cu(C_4H_3S)]$, it is interesting to note that the active Se atom is released from the $[WSe_4]^{2-}$ anion and is inserted into the Cu–C bond of the $Cu(C_4H_3S)$ moiety to afford the 2-selenothophene ligand. Then the complex $CuSe(C_4H_3S)$ coordinates with the $[Et_4N]_2[WSe_4]$ to form a novel linear trinuclear cluster compound $[Et_4N]_2[(\mu\text{-}WSe_4)\{(SC_4H_3)SeCu\}_2]$ [13]. The geometry about the Cu atom is roughly trigonal with the angle of the metal-bridging Se atoms being significantly less than the angles of the inserted Se atom. Bond lengths for the Cu and metal-bridging Se atoms (2.331(2) and

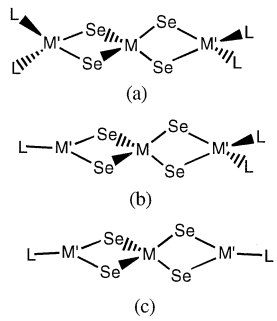

Fig. 3. Three types of structural modes of trinuclear linear heteroselenometallic clusters (M = Mo or W; M′ = Cu, Ag or Au; L = ligands).

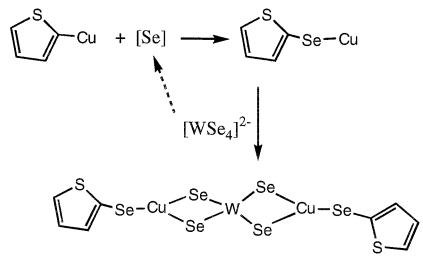

Fig. 4. Selenium insertion reaction and cluster coordination reaction.

2.336(2) Å) are obviously longer than the $Cu–Se_{insertion}$ bond length (2.284(2) Å) (Fig. 4).

Tetranuclear cubane-like cluster compounds were isolated easily from the reactions of $[M(PR_3)]^+$ (M = Cu, Ag; R = Ph, $PhMe_2$, *t*-Bu) with the $[MSe_4]^{2-}$ anion in a 3:1 Cu(Ag):M ratio in the presence of a halides, suggesting that the cubane-like structure is quite stable [10,15,28]. In fact, these kinds of clusters are not only air- and moisture-stable, but also photo-stable in the solid state as well as in solution [29]. The stability of these cubane-like clusters may be due to weak interactions between Cu(I) or Ag(I) and halides. The average Cu(Ag)–X interatomic distance increases on going from Cl^- to I^-. Interestingly, two types of Cu–X distance are found in the Cu-containing cubane-like cluster (one short and two long bonds), while the Ag-containing cubane-like clusters have three long Ag–X bonds [28,30]. The distortion of the cubane-like structure for $\{MM'_3Se_3X\}(PR_3)(Se)$ (M = Mo, W; M′ = Cu, Ag) is dependent upon the halide located at one vertex of the cubane core $\{MM'_3Se_3X\}^{2+}$ (see Fig. 5).

The average Cu(Ag)–X–Cu(Ag) bond angle deviates from 90° and decreases on going from Cl^- to I^-. The utility of the cubane-like $\{MM'_3Se_3X\}^{2+}$ as a promising synthon to construct polynuclear clusters with novel structural modes is a very fertile area. For instance, reaction of $[(\mu_3\text{-}WSe_4)(\mu_3\text{-}Cl)(CuPPh_3)_3]$ with Li_2Se in the presence of $[Et_4N]\cdot Cl$ yielded a pinwheel-shaped cluster $[Et_4N]_4[(\mu\text{-}WSe_4)_3(Cu_3)_2(\mu_3\text{-}Se)_2]$ (see below) [31]. Also, if the cubane-like clusters $\{MM'_3Se_3X\}(PPh_3)(Se)$ ($M = Mo$, W; $M' = Cu$, Ag) are treated with a little water, the O atom of water may slowly substitute the terminal Se atom of the cluster. Only a few clusters with a terminal Mo–O bond have been reported [12,32].

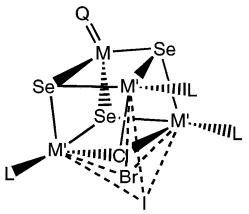

Fig. 5. Structural sketch of the typical cubane-like cluster, the difference in halide ion is shown (M = Mo or W; M′ = Cu or Ag; Q = O or Se).

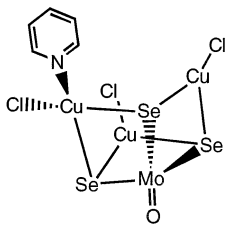

Fig. 6. Structural sketch of the $[(\mu_3\text{-}MoOSe_3)Cu_3Cl_3(py)]^{2-}$ anion.

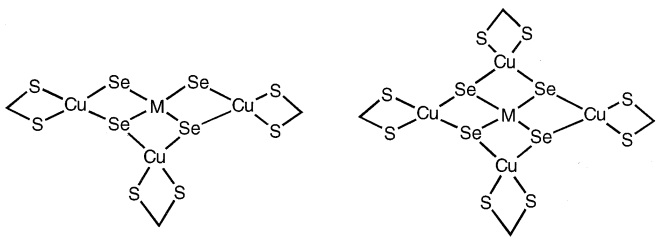

Fig. 7. Two structural types of heteroselenometallic clusters with dithiocarbamate ligands: (a) $[(\mu_3\text{-}MSe_4)(Et_2NCS_2Cu)_3]^{2-}$ and (b) $[(\mu_4\text{-}MSe_4)(Me_2NCS_2Cu)_4]^{2-}$ (M = Mo or W).

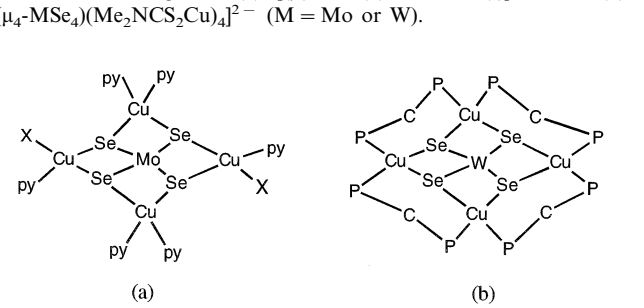

Fig. 8. Structural sketches of heteroselenometallic clusters with MCu_4 core cross-frame: (a) $[(\mu_4\text{-}MoSe_4)Cu_4(py)_6Cl_2]$, (b) $[(\mu_4\text{-}WSe_4)\{Cu(dppm)\}_4]^{2+}$.

To date only one example of a heteroselenometallic cluster, $[Ph_4P]_2[(\mu_3\text{-}MoOSe_3)Cu_3Cl_3(py)]$ which has a structural type similar to the incomplete cubane, has been reported [33]. The structure of $[(\mu_3\text{-}MoOSe_3)\text{-}Cu_3Cl_3(py)]^{2-}$ shown in Fig. 6 consists of an open-nest shaped $MoCu_3Se_3$ core. There are two kinds of Cu atoms: (a) the tetrahedral Cu atom coordinates to two Se, one Cl and one N of py; (b) the trigonal Cu atom bonds to two Se and one Cl atom.

Treatment of $[Et_4N]_2[MSe_4]$ with CuCl and $R_2NCS_2\text{-}Na$ (R = Et, $PhCH_2$ or $R_2 = C_4H_8$, C_5H_{10}) resulted in the formation of tetranuclear clusters $[Et_4N]_2[(\mu_3\text{-}MSe_4)(R_2NCS_2Cu)_3]$. Intriguingly, with Me_2dtcNa, the pentanuclear clusters $[Et_4N]_2[(\mu_4\text{-}MSe_4)(Me_2NCS_2Cu)_4]$ were isolated [19,34]. The formation of pentanuclear clusters may be attributed to the smaller steric demand and stronger σ–π conjugation effect of the methyl group in $Me_2NCS_2^-$ than other large alkyl groups in $R_2NCS_2^-$. This gives rise to stabilization of the cluster containing Me_2dtcM units and leads to a variety of novel cluster structures [35]. The structural types of the cluster anions $[(\mu_3\text{-}MSe_4)(Et_2NCS_2Cu)_3]^{2-}$ and $[(\mu_4\text{-}MSe_4)(Me_2NCS_2Cu)_4]^{2-}$ (shown in Fig. 7) are different. However, it is noteworthy that the metal atoms in both the MCu_3 and MCu_4 cores are nearly coplanar. The dialkyldithiocarbamate ligands and the coordination geometries of the Cu atoms seem to have little effect on the Cu–Se bond lengths in these heteroselenometallic clusters.

Similar to pentanuclear planar MCu_4 sulfur cluster compounds containing mixed ligands py and halide or pseudo-halide, the clusters $[(\mu_4\text{-}MSe_4)Cu_4(py)_6X_2]$ (X = Cl, Br, CN and SCN) may be easily synthesized from the reaction of $[Et_4N]_2[MSe_4]$ with CuX in a DMF/py mixture, in which py acts as both a ligand and a co-solvent [13,36]. The structure of $[(\mu_4\text{-}MoSe_4)Cu_4\text{-}(py)_6Cl_2]$, as shown in Fig. 8a, is composed of a $MoSe_4$ moiety coordinated by four Cu atoms with chloride and pyridine mixed ligands. Another pentanuclear WCu_4 cross-planar cluster compound $[(\mu_4\text{-}WSe_4)\{Cu\text{-}(dppm)\}_4][ClO_4]_2$ was prepared by the reaction of $[Cu(MeCN)_4][ClO_4]$ with $[Et_4N]_2[WSe_4]$ in the presence of excess dppm [37]. This preparation seems specific for the dppm ligand, as similar clusters were not obtained with PPh_3 or dppe. The structure of the cluster cation $[(\mu_4\text{-}WSe_4)\{Cu(dppm)\}_4]^{2+}$ (Fig. 8b) is different from that of the sulfuric analog $[(\mu_3\text{-}WS_4)\{Cu(dppm)\}_3]^+$ [38]. Four copper atoms are bound to the WSe_4 moiety in which each is symmetrically attached to one edge of the tetrahedral, and are in a square arrangement in

which each edge is doubly bridged by a dppm ligand. It is interesting to note that the six-membered ring comprising a dppm ligand, two chelated adjacent Cu atoms and the bridging Se atom has a distorted chair formation. Four such six-membered rings are around $[WSe_4]^{2-}$ anion. The average W–Cu separation is 2.815(8) Å.

Two different routes are available for the synthesis of the undecanuclear cage-shaped cluster anion $[(\mu_6\text{-}MoSe_4)Cu_{10}(\mu\text{-}SPh)_{12}]^{4-}$. When $[Et_4N]_2[(CN)Cu(\mu\text{-}Se)_2Mo(\mu\text{-}Se)_2Cu(CN)]$ reacts with $[Et_4N]_2[Cu(PhS)_3]$, $[Et_4N]_4[(\mu_6\text{-}MoSe_4)Cu_{10}(\mu\text{-}SPh)_{12}]$ is obtained in a relatively high yield. The same product is also obtained from the reaction of $[Et_4N]_2[MoSe_4]$ with excess $[Et_4N]_2[Cu(PhS)_3]$. The final product can be easily isolated because of the high solubility of the thiophenolate-containing cluster [19]. The inner core $\{MoSe_4Cu_6\}$ of the cluster anion $[(\mu_6\text{-}MoSe_4)Cu_{10}(\mu\text{-}SPh)_{12}]^{4-}$ (illustrated in Fig. 9) consists of a central $MoSe_4$ tetrahedron encapsulated by six tetrahedral-coordinated Cu atoms across the six edges of the $MoSe_4$ moiety. The other four trigonally coordinated Cu atoms are attached to this core by 12 μ-SPh bridging ligands. The four Mo–Se distances are equal to 2.378(2) Å, which is slightly longer than those in other selenomolybdate cluster compounds. The average Mo–Cu separation is 2.856(3) Å.

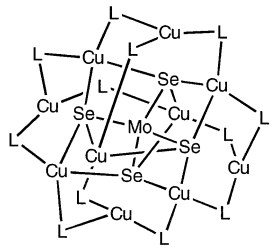

Fig. 9. Structure of the cage-shaped cluster anion $[(\mu_6\text{-}MoSe_4)Cu_{10}(\mu\text{-}SPh)_{12}]^{4-}$.

$[WSe_4]^{2-}$ with $Ni(acac)_2$ would be expected to produce $[Ni(WSe_4)_2]^{2-}$. Similarly reaction of $PdCl_2(PhCN)_2$ with $[PPh_4]_2[WSe_4]$ afforded $[PPh_4]_2[Pd(WSe_4)_2]$ [23]. X-ray powder photography indicated that $[PPh_4]_2[Pd(WSe_4)_2]$ and $[PPh_4]_2[Ni(WSe_4)_2]$ are isostructural. In the $[Ni(WSe_4)_2]^{2-}$ anion, the Ni center is square-planar and bonded to two slightly distorted tetrahedral WSe_4 groups. The average Ni–W and Ni–Se bond distances are 2.866(1) and 2.350(1) Å, respectively (Eq. (4)).

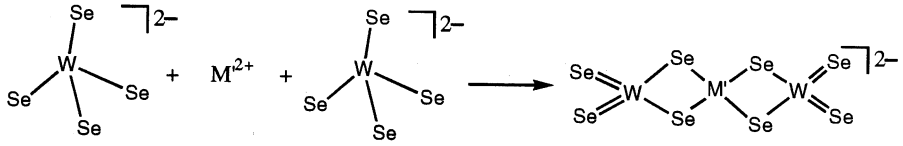

(4)

Treatment of $[Et_4N]_2[WSe_4]$ with $[Pd_2(\mu\text{-}dppm)_2Cl_2]$ in a CH_2Cl_2–DMF mixture solvent afforded a novel neutral heterohexanuclear palladium(I) cluster $[(\mu_3\text{-}WSe_4)_2(Pd_2)_2(\mu\text{-}dppm)_2]\cdot 2DMF$ which was formed by displacement of two chlorides and one dppm ligand in complex $[Pd_2(dppm)_2]Cl_2$, and by two $[WSe_4]^{2-}$ anions [40] (Eq. (5)).

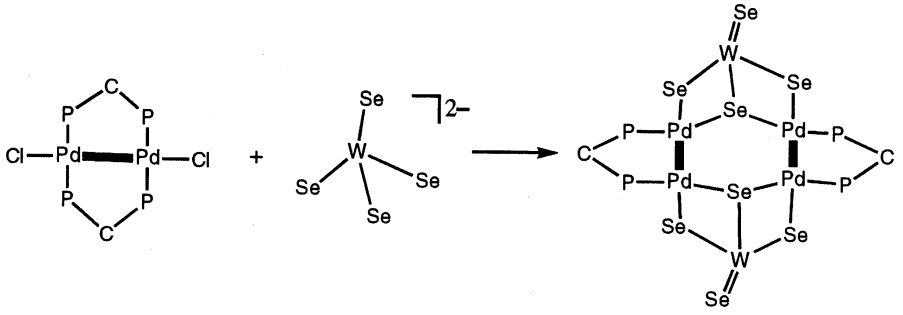

(5)

Each palladium atom is asymmetrically surrounded by one μ_3-Se, one μ-Se, one Pd and one P atom, forming a highly distorted square-planar arrangement. The dppm bridging the Pd–Pd distance is similar to that of $[Pd_2(\mu\text{-}dppm)_2Cl_2]$, indicating that the cluster still belongs to the so-called class of A-frame compounds [41]. Due to strong d–p hybridization between the Pd and μ_3-Se atoms the average Pd–μ_3-Se bond length is slightly shorter than the average Pd–μ-Se bond length. The average W–Pd separation is 2.9439(8) Å.

2.2. Poly-Mo(W) center cluster compounds

Müller et al. reported a series of anionic mixed-metal sulfides $[M'(MS_4)_2]^{2-}$ (M = Mo, W; M′ = Fe, Co, Ni, Pd, Pt, Zn, Cd, Hg) [39]. These anions all feature two nearly tetrahedral, bidentate MS_4 units bound to a M′ center. The coordination geometry about the central metal can be tetrahedral or square planar. On the basis of the mixed-metal sulfide chemistry, reaction of

Reaction of $FeCl_3$ with $[MSe_4]^{2-}$ (M = Mo, W) in the presence of a monodentate thiolate ligand led to a 'self-assembly' type process and the formation of double-cubane clusters. Stiefel has reported three types of selenide-containing double-cubane clusters, of which two were structurally characterized by single-crystal X-ray diffraction [42]. The 'self-assembly' of double-cubane clusters using the substitutionally labile monodentate thiolate ligands is based upon methods developed by Holm for the analogous sulfur clusters [43].

$$[MSe_4]^{2-} + 3.5FeCl_3 + (9 \sim 12)NaSEt \rightarrow \begin{matrix}[M_2Fe_6Se_8(SEt)_9]^{3-} \\ [M_2Fe_7Se_8(SEt)_{12}]^{3-}\end{matrix} \quad (6)$$

$$[M_2Fe_7Se_8(SEt)_{12}]^{3-} + 6HSAr \rightarrow [M_2Fe_7Se_8(SEt)_6(SAr)_6]^{3-} \quad (7)$$

Similar to their $[MS_4]^{2-}$ analogs, the $[MSe_4]^{2-}$ anions reacted with Fe(III) salts to give the corresponding selenium double-cubane clusters. This indicates that $[MSe_4]^{2-}$ can effectively deliver all four selenium atoms in the assembly process even though one of the selenium atoms is no longer covalently bound to the central M atom. Further investigation showed that the single-cubane clusters were formed by a similar spontaneous assembly process when $[MoSe_4]^{2-}$ reacted with $FeCl_2$ in the presence of bidentate thiolate ligands [44].

$$[MoSe_4]^{2-} + 3FeCl_2 + 6NaS_2CNR_2 \rightarrow MoFe_3Se_4(S_2CNR_2)_6 \ (R = Me, Et) \quad (8)$$

The structure of the anions in both $[M_2Fe_6Se_8(SEt)_9]^{3-}$ and $[M_2Fe_7Se_8(SEt)_6(SC_6H_4Cl)_6]^{3-}$ is of the 'double-cubane' type containing trigonally distorted $MoFe_3Se_4$ subclusters which are linked through the Mo atoms. In the former, linkage between two $MoFe_3Se_4$ subclusters is by three μ-ethanethiolate ligands; in the latter, the bridge is accomplished by a $Fe(SEt)_6$ distorted trigonal anti-prismatic moiety. The structures, as shown in Fig. 10, are similar to the analogous sulfur double-cubanes, with the major structural difference being the more acute bridging Mo–Fe–Se angles within the $MoFe_3Se_4$ subclusters. The mean Mo–Se bond distance of 2.490(4) Å and the mean Fe–Se bond distance of 2.388(8) Å are 4% longer than the mean Mo–S (2.357(7) Å) and Fe–S (2.270(12) Å) distances in the corresponding sulfur clusters. In the sulfur analog the mean Mo–Fe–S angle is 72.4°, whereas in the selenium analog it is diminished to 69.3°. This observation suggests that the stability of the $MoFe_3Se_4$ cubane subcluster may be enhanced by the maintenance of an optimum metal-to-metal distance with the cubane [42]. No statistically significant variation in the Fe–Se bond lengths of Fe-containing heteroselenometallic clusters is observed in accord with a delocalized model with formally $Fe^{2.67+}$ ions, as opposed to a localized model with Fe^{3+} and Fe^{2+} ions.

Although cubane-like clusters are well known, their reaction chemistry has not been well probed. Only one example has been reported of a reaction involving a cubane-like cluster as a building block for novel clusters [31]. Treatment of $[(\mu_3\text{-}WSe_4)(\mu_3\text{-}Cl)(CuPPh_3)_3]$ in DMF with Li_2Se in the presence of $[Et_4N]\cdot Cl$ affords the novel cluster $[Et_4N]_4[(\mu_3\text{-}WSe_4)_3(Cu_3)_2(\mu_3\text{-}Se)_2]$ (Fig. 11). The precipitation of LiCl, heat, and insolubility of the $[Et_4N]^+$ salt of the cluster anion provide the driving force for this reaction. The cubane is opened upon reaction with Se^{2-} and these remnants are linked by Se atoms. The structure frame of the $[(\mu_3\text{-}WSe_4)_3(Cu_3)_2(\mu_3\text{-}Se)_2]^{4-}$ anion looks like a 'pinwheel' shape, which consists of two Cu_3 triangles bridged by the tridentate $[WSe_4]^{2-}$ moieties and capped by two μ_3-Se atoms. The Cu–Cu distances within the equilateral Cu_3 triangles have an average value of 2.880(3) Å, while others between the eclipsed Cu_3 triangles range from 3.518(3) to 3.580(3) Å. The average W–Cu separation of 2.738 Å in the WSe_4Cu_2 moiety is shorter than that in the cubane cluster (2.753(3) Å) [10].

The reaction in DMF of $PbCl_2$ or $SnCl_2$ with $[NH_4]_2[WSe_4]$ in the presence of $[PPh_4]Br$ yielded the clusters $[PPh_4]_4[M_2(WSe_4)_4]$ (M = Pb, Sn). The structure

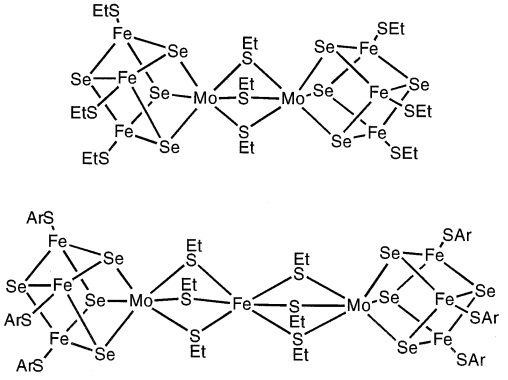

Fig. 10. Structural sketches of two Mo–Fe–Se double-cubane cluster anions: $[Mo_2Fe_6Se_8(SEt)_9]^{3-}$ (up) and $[Mo_2Fe_7Se_8(SEt)_6(SC_6H_4Cl)_6]^{3-}$ (down).

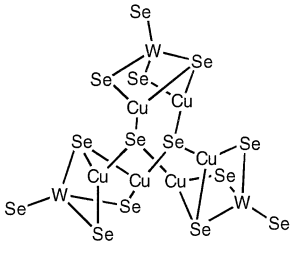

Fig. 11. Structural sketch of a pinwheel-shaped cluster anion $[(\mu_3\text{-}WSe_4)_3(Cu_3)_2(\mu_3\text{-}Se)_2]^{4-}$.

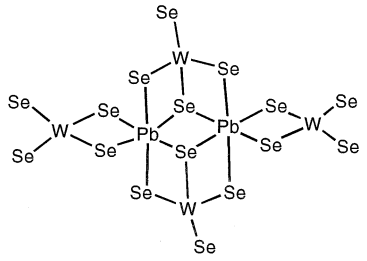

Fig. 12. Sketch of the structure of the $[Pb_2(WSe_4)_4]^{4-}$ anion.

of $[PPh_4]_4[Pb_2(WSe_4)_4]$ was determined by X-ray crystallography [45]. The $[Pb_2(WSe_4)_4]^{4-}$ anion consists of two distorted $PbSe_6$ edged-shared octahedra (Fig. 12). There are two crystallographically distinct W atoms in this structure. Each is tetrahedrally coordinated by four Se atoms. One WSe_4 tetrahedron is edge shared to a $PbSe_6$ octahedron while the other contributes the Se vertices that are edge shared between $PbSe_6$ octahedron. The distances from Pb to μ_2-Se are 2.904(1) to 3.121(1) Å, which are shorter than those to the μ_3-Se atoms (3.124(1)–3.185(1) Å). No bonding interactions are found between W and Pb atoms.

Although a few heterometallic polymeric clusters of tetrathiometalates have been isolated and structurally characterized [46], the corresponding clusters of tetraselenometalates have not been extensively investigated. Two polymeric clusters containing the $[WSe_4]^{2-}$ anion were synthesized and structurally characterized in our laboratory [20]. $[PPh_4]_2[WSe_4]$ reacts with an equal equivalent of $[Ag(MeCN)_4][ClO_4]$ in DMF to afford a linear polymeric cluster $\{[Ph_4P][(\mu\text{-}WSe_4)Ag]\}_n$. Treatment of $\{[Ph_4P][(\mu\text{-}WSe_4)Ag]\}_n$ with excess $La(NO_3)_3 \cdot 3H_2O$ in DMSO solution resulted in the formation of a helical chain polymeric cluster $\{[La(Me_2SO)_8][(\mu\text{-}WSe_4)_3Ag_3]\}_n$ [20]. The transformation of the anion cluster skeletons originates from the correlation of the cation counterion size by the self-assembly reaction in the solution. The macroanions $[(\mu\text{-}WSe_4)_3Ag_3]^{3-}$ form an infinite one-dimensional chain running parallel to the monoclinic symmetric axis. The basic repeating unit is a butterfly-type $SeWSe_3Ag_2$ containing the bridging $\mu\text{-}WSe_4^{2-}$ group, which is linked through interactions with the Ag atom of one fragment and Ag atom of another to form an intriguing helical array of repeating $[(\mu\text{-}WSe_4)_3Ag_3]^{3-}$ cluster units. Fig. 13 shows a view of an individual chain. This chain is made up of two sets of helices which propagate alternately along the chain.

The CuCN, KCN and $[Et_4N]_2[WSe_4]$ reaction system either in DMF/2-picoline or in the solid state at 80°C resulted in the formation of a novel three-dimensional cluster $\{[Et_4N]_2[(\mu_4\text{-}WSe_4)Cu_4(CN)_4]\}_n$ [20]. The $[Cu(CN)_2]^-$ anionic species is the key to the formation of the polymeric cluster in the reaction. The framework of the polymeric anion, as shown in Fig. 14, is constructed from the WSe_4Cu_4 units bridged by cyanide ligands. In the WCu_4 core, five metal atoms are entirely co-planar with the Cu–W–Cu angles of 180° concerning the two mutually *trans* Cu atoms, which forms an ideal crystallographic D_{2d} symmetry for the WSe_4Cu_4 aggregate. Two *cis* Cu atoms have a distorted tetrahedral geometry with their tetrahedral apices occupied by two triply bridging Se atoms and two cyanide bridging C or N atoms, forming a $CuSe_2C_2$ or $CuSe_2N_2$ unit, respectively. These two kinds of tetrahedra are mutually linked by bridging cyanide ligands, thus forming a polymeric three-dimensional network of the basic formula $\{[(\mu_4\text{-}WSe_4)Cu_4(CN)_4]^{2-}\}_\infty$.

3. Spectroscopy

3.1. UV–vis and IR spectroscopy

Although both electronic and infrared spectroscopies are of use in the characterization of soluble metal sulfides [5,6], their application to the characterization of soluble metal selenides is limited. The problem associated with IR spectroscopy is that M–Se (M = Mo, W) bond stretching vibrations often show absorption in the range 200–400 cm^{-1} in the far-IR region. Thus, one should be cautious in assigning these bands in view of other vibrational absorptions in the lower wavenumbers. Most of the heteroselenometalates synthesized until now show intense bands in their electronic absorption spectra. The UV–vis electronic spectra are useful for primitive identification but not for definitive characterization. A possible reason may be due to the fact that the greater spin orbit coupling of the heteroselenometalates compared with the thiometalates makes interpretation of the UV–vis data much more difficult. So, in contrast to NMR spectroscopy, UV–vis and IR

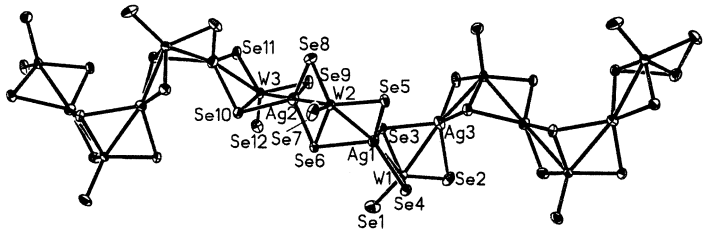

Fig. 13. A view of the structure of the polymeric anion $\{[(\mu\text{-}WSe_4)_3Ag_3]^{3-}\}_n$ with three repeating units.

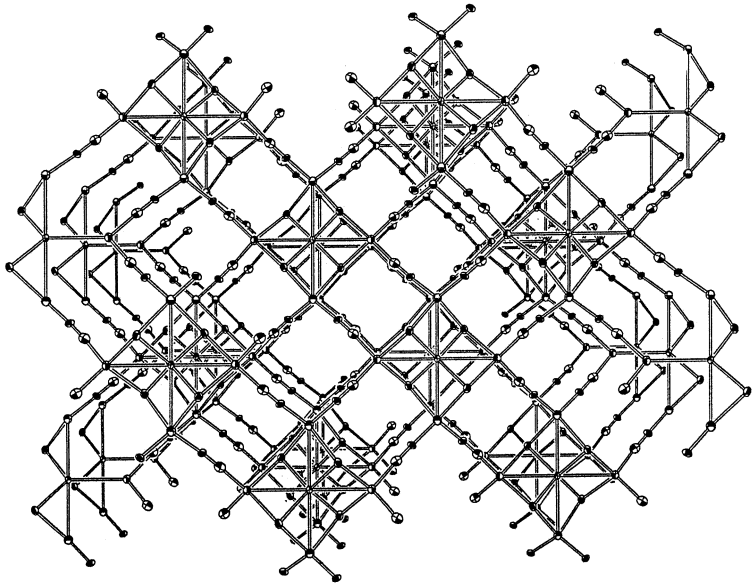

Fig. 14. A perspective view of the polymeric anion $\{[(\mu_4\text{-}WSe_4)Cu_4(CN)_4]^{2-}\}_\infty$. (Reprinted by permission from Inorg. Chem. 39 (2000) 423. Copyright 2000 ACS.)

spectroscopies of heteroselenometalates were not extensively discussed in the literature [10,16,19].

However, the UV–vis electronic spectra of $[MSe_4]^{2-}$ (M = Mo, W) were studied by Müller in 1981 [5]. The visible absorption maxima are red shifted 60–80 nm in the selenides compared with those for the corresponding sulfides. The possible reason is that there is a greater orbital overlap in the selenometalates than in the thiometalates due to the larger covalent radius of the selenium atom relative to sulfur. All heteroselenometallic clusters have intense bands in their electronic absorption spectra, typically a broad peak in the 450–490 nm range and a less intense band between 320–380 nm. With reference to the electronic spectra of the free $[MSe_4]^{2-}$ anions, absorption bands in this region have been assigned as charge-transfer bands of the type ($\pi(Se) \rightarrow d(M)$) arising from the MSe_4 moieties. A relatively weak $[MSe_4]^{2-}$ to coordinated metal interaction may be inferred from a comparison of the band positions for heteroselenometallic clusters with those for free $[MSe_4]^{2-}$ anions [10,23]. The absorption bands for heteroselenometalates are observed at higher energies than those for the $[MSe_4]^{2-}$ anions, indicative of strong interactions between the coordinated-metal and the $[MSe_4]^{2-}$ anion moiety. Additionally, the $Se \rightarrow M$ charge-transfer bands are blue shifted by ca. 40 nm when Mo is replaced by W in the clusters [47]. This is expected for LMCT, owing to the higher optical electronegativity of Mo^{VI} versus W^{VI} [48]. A very intense band in the range 250–300 nm is tentatively attributed to an intraligand transition from the peripheral ligands of the clusters.

The Mo–Se stretching vibrations for heteroselenometallic clusters occur in the range 300–380 cm^{-1}, while the corresponding W–Se stretches are shifted to even lower energies. The $\nu(Mo\text{–}Se_t)$ (terminal) vibrations at 375–380 cm^{-1} for cubane-like selenomolybdate clusters are higher than that for the free $[MoSe_4]^{2-}$ moiety (ca. 341 cm^{-1}), whereas $\nu(Mo\text{–}Se_b)$ (bridging) were found at lower energies (ca. 330–320 cm^{-1}) [49]. The wavenumbers for $\nu(Mo\text{–}Se_b)$ are related to the number of Se-bridges. In fact, it is not difficult to understand that the difference in $\nu(Mo\text{–}Se)$ should parallel the change in Mo–Se bond length. For example, in $[(MoSe_4)(AuPPh_3)_2]$, $\nu(Mo\text{–}\mu\text{-}Se_b)$ is found at 338 cm^{-1} and the corresponding $d(Mo\text{–}\mu\text{-}Se_b)$ is 2.344(2) Å [25]; in $[(MoSe_4)(AgPPh_3)_3Cl]$, $\nu(Mo\text{–}\mu_3\text{-}Se_b)$ is found at 326 cm^{-1} and $d(Mo\text{–}\mu_3\text{-}Se_b)$ is 2.364(2) Å [30b]; in $[Et_4N]_4[MoCu_{10}Se_4(PhS)_{12}]$, $\nu(Mo\text{–}\mu_4\text{-}Se_b)$ is found at 292 cm^{-1} and $d(Mo\text{–}\mu_4\text{-}Se_b)$ is 2.378(2) Å [19]. For selenotungstate clusters, the $\nu(W\text{–}Se)$ frequencies are found in the expected range 280–310 cm^{-1}. With reference to $\nu(W\text{–}Se)$ absorption of the free $[WSe_4]^{2-}$ at 305 cm^{-1} [5], the $\nu(W\text{–}Se)$ stretching modes in the selenotungstate clusters have a smaller shift than in the selenomolybdate clusters [34]. IR spectroscopy may be used to confirm the presence of peripheral ligands such as PPh_3, py and $R_2NCS_2^-$ in the clusters. There is no overlap between the typical IR bands for these ligands and $\nu(M\text{–}Se)$.

3.2. NMR spectroscopy

Incontrast to electronic and infrared spectroscopies, NMR spectroscopy can provide very useful characterization of heteroselenometallic clusters. Table 2 lists ^{77}Se, ^{95}Mo and ^{31}P NMR data for some heteroselenometallic clusters. No ^{183}W NMR results of seleno-

Table 2
Multinuclear NMR spectroscopic data for heteroselenometallic clusters [a]

Species	^{77}Se (δ ppm)	^{95}Mo (δ ppm)	^{31}P (δ ppm)	Reference
$[MoSe_4]^{2-}$	t 1643 [b]	3339 [c]		
$[WSe_4]^{2-}$	t 1235			[50b]
$[(NC)Cu(\mu\text{-}Se)_2MoSe_2]^{2-}$	t 1832, b 1030			[14]
$[(NC)Cu(\mu\text{-}Se)_2WSe_2]^{2-}$	t 1383, b 782			[14]
$[(\mu\text{-}MoSe_4)\{Cu(CN)\}_2]^{2-}$	b 1195			[14]
$[(\mu\text{-}WSe_4)\{Cu(CN)\}_2]^{2-}$	b 920			[14]
$[(\mu\text{-}WSe_4)\{(SC_4H_3)SeCu\}_2]^{2-}$	b 906, o −18.1			[13]
$[(Se_2)Ni(\mu\text{-}Se)_2WSe_2]^{2-}$	t 1399,b 855,mbr 608			[23]
$[Se_2W(\mu\text{-}Se)_2Ni(\mu\text{-}Se)_2WSe_2]^{2-}$	t 1628, b 994			[23]
$[Se_2W(\mu\text{-}Se)_2Pd(\mu\text{-}Se)_2WSe_2]^{2-}$	t 1673, b 1135			[14]
$[Se_2W(\mu\text{-}Se)_2Pt(\mu\text{-}Se)_2WSe_2]^{2-}$	t 1627, b 949			[14]
$[(\mu\text{-}WSe_4)\{Cu(Me_2PhP)\}_2]$	b 1044		−40.1	[10]
$[(\mu\text{-}WSe_4)\{Ag(Me_2PhP)\}_2]$	b 1092		−36.0	[10]
$[(\mu\text{-}WSe_4)\{Au(Me_2PhP)_2\}_2]$	b 1234		−34.3	[10]
$[(\mu\text{-}WSe_4)\{Au(MePh_2P)\}_2]$	b 1244		−20.5	[10]
$(\mu_3\text{-}Cl)(\mu_3\text{-}WSe_4)[(PPh_3)Cu]_3$	t 1651, b 1232		24.7	[10]
$(\mu_3\text{-}Cl)(\mu_3\text{-}MoSe_4)[(PPh_3)Cu]_3$		1303	14.0	[30a]
$(\mu_3\text{-}Cl)(\mu_3\text{-}MoSe_4)[(PBu^t_3)Cu]_3$			23.6	[54]
$(\mu_3\text{-}Br)(\mu_3\text{-}MoSe_4)[(PPh_3)Cu]_3$		1301	12.7	[30a]
$(\mu_3\text{-}I)(\mu_3\text{-}MoSe_4)[(PPh_3)Cu]_3$		1316	9.38	[30a]
$(\mu_3\text{-}Cl)(\mu_3\text{-}MoSe_4)[(PPh_3)Ag]_3$		1377	3.57	[25]
$(\mu_3\text{-}Br)(\mu_3\text{-}MoSe_4)[(PPh_3)Ag]_3{\cdot}SePPh_3$		1372	3.12, 35.9 [d]	[30b]
$(\mu_3\text{-}Br)(\mu_3\text{-}WSe_4)[(PPh_3)Ag]_3$	t 1674, b 1182		5.47	[20]
$(\mu_3\text{-}Cl)(\mu_3\text{-}WSe_4)[(PPh_3)Ag]_3{\cdot}SePPh_3$			5.21, 35.8 [d]	[26b]
$(PPh_3)Cu(\mu\text{-}Se)_2Mo(\mu\text{-}Se)_2Cu(PPh_3)_2$		2323	13.7, 11.2	[25]
$(PPh_3)Ag(\mu\text{-}Se)_2Mo(\mu\text{-}Se)_2Ag(PPh_3)_2$		2407	3.45, 3.14	[25]
$(PPh_3)Cu(\mu\text{-}Se)_2W(\mu\text{-}Se)_2Cu(PPh_3)_2$			26.7, 28.0	[26b]
$(PPh_3)Ag(\mu\text{-}Se)_2W(\mu\text{-}Se)_2Ag(PPh_3)_2$			3.74, 3.91	[26b]
$(\mu\text{-}MoSe_4)[(PPh_3)Ag]_2$		2429	5.92	[25]
$(\mu\text{-}MoSe_4)[(PPh_3)Au]_2$		2326	53.0	[25]
$(\mu\text{-}WSe_4)[(PPh_3)Au]_2$			52.5	[26b]
$[(\mu_3\text{-}MoSe_4)(Et_2NCS_2Cu)_3]^{2-}$		2086		[19]
$[(\mu_4\text{-}MoSe_4)(Me_2NCS_2Cu)_4]^{2-}$		−1.50		[19]
$[(\mu_4\text{-}WSe_4)Cu_4Br_2(py)_6]$	b 742			[20]
$[(\mu_6\text{-}MoSe_4)Cu_{10}(\mu\text{-}SPh)_{12}]^{4-}$		−1.30		[19]
$\{[(\mu\text{-}WSe_4)_3Ag_3]^{3-}\}_n$	t 1612, b 953 792			[20]

[a] Key: t terminally bonded Se atom; b bridging Se atom; mbr metal-bound ring Se atom; o Se atom bound to organic fragment.
[b] Ref. [49].
[c] Ref. [52].
[d] This chemical shift is due to $SePPh_3$.

tungstate clusters have been reported, although ^{183}W is an NMR active nucleus (spin 1/2, natural abundance 14.3%). The ^{1}H NMR absorption signals for the diamagnetic heteroselenometallic clusters are very close to those for the free ligands and cations.

Selenium has a spin-half nucleus with moderate NMR receptivity (for ^{77}Se: $I = 1/2$, natural abundance 7.58%, receptivity relative to ^{13}C 2.98) and can be studied by NMR spectroscopy. Ibers and coworkers' studies have shown that the ^{77}Se NMR chemical shifts for soluble transition-metal selenide compounds have a wide range from 100 to 2200 ppm [9a,50]. With this scale of ^{77}Se chemical shift established, ^{77}Se NMR spectroscopy has become an important analytical tool for soluble transition-metal selenide chemistry. In the closed d^{10} coinage-metal clusters $(\mu\text{-}WSe_4)[(PMe_2Ph)_2M']$ (M = Cu, Ag and Au), the ^{77}Se resonances shift downfield on going from Cu^+ to Au^+, a trend that can be ascribed to a smooth increase in M′–Se orbital overlap [10]. The resonances for bridging and terminal selenide groups in the cubane-like and linear dinuclear clusters are shifted upfield and downfield, respectively, compared with that for the free $[WSe_4]^{2-}$ ($\delta_{Se} = 1235$ ppm). For example, two peaks are found as expected in the ^{77}Se NMR spectrum of $(\mu_3\text{-}Cl)(\mu_3\text{-}WSe_4)[(PPh_3)Cu]_3$, one at 1651 ppm arising from the terminal Se and the other at 1232 ppm from the Se nuclei in the cubane core [10]. A similar trend is observed in the selenomolybdate compound $[PPh_4]_2[(NC)Cu(\mu\text{-}Se_2)MoSe_2]$ ($\delta(Se_t) = 1820$ ppm, $\delta(Se_b) = 1030$ ppm) by comparison with $[MoSe_4]^{2-}$ ($\delta = 1643$ ppm) [14]. Interestingly, the chemical shifts of the equivalent Se_b atoms in symmet-

ric cluster anions such as $[(NC)Cu(\mu\text{-}Se_2)W(\mu\text{-}Se_2)Cu(CN)]^{2-}$ ($\delta(Se_b) = 920$ ppm) and $[(NC)Cu(\mu\text{-}Se_2)Mo(\mu\text{-}Se_2)Cu(CN)]^{2-}$ ($\delta(Se_b) = 1195$ ppm) are higher than those in the asymmetric cluster anions such as $[(NC)Cu(\mu\text{-}Se_2)WSe_2]^{2-}$ ($\delta(Se_b) = 782$ ppm) and $[(NC)Cu(\mu\text{-}Se_2)MoSe_2]^{2-}$ ($\delta(Se_b) = 1030$ ppm) [14]. Thus, the Se_b atoms are shielded and the Se_t atoms are deshielded with respect to the Se_b nuclei in the symmetric anions.

Since the heterometals among the heteroselenometallic clusters are different, it is not surprising that a large difference in their ^{77}Se chemical shifts is observed. For clusters with the same metal in a different coordination environment, the difference in their chemical shifts is also obvious. In the open d-shell metal clusters $[PPh_4]_2[Se_2W(\mu\text{-}Se_2)M'(\mu\text{-}Se_2)WSe_2]$ ($M' = Ni$, Pd and Pt), the central heterometal affects the chemical shifts of both bridging and terminal Se atoms. The resonance for a Se bonded to a third-row transition metal is usually more upfield than that for a Se bonded to a second-row transition metal. Thus, the ^{77}Se chemical shifts for the Pd-containing cluster anion are downfield from those for the Ni or Pt congener [23]. In addition, the heterometal affects the chemical shift for the Se_b atoms more than that for the Se_t atoms, presumably because of the closer proximity to the Se_b atoms. This trend is different from that for close d-shell coinage-metal clusters. The ^{77}Se NMR spectrum of $[Et_4N]_2[(\mu\text{-}WSe_4)\{CuSe(SC_4H_3)\}_2]$ shows two resonances: a peak at 905.8 ppm is due to metal-bridging Se atoms and a peak at -18.1 ppm is attributable to Se atoms bearing organic substituents [13]. As expected, three peaks at δ 1612, 953, and 792 ppm were found in the ^{77}Se NMR spectrum of $\{[La(Me_2SO)_8][(\mu\text{-}WSe_4)_3Ag_3]\}_n$, which are tentatively assigned to the terminal Se, the bridging μ-Se and μ_3-Se, respectively. The ^{77}Se NMR spectrum of $[(\mu_4\text{-}WSe_4)Cu_4(CN)_2(py)_4]$ exhibits a broad singlet at 742 ppm which arises from the μ_4-Se atoms [20]. The ^{77}Se NMR spectrum of $[PPh_4][(Se_2)Ni(WSe_4)]$ shows three resonances at δ 1399, 855, and 608 ppm, suggesting that there are three types of Se environment: terminal Se bonded to W and two kinds of bridging Se bound to W and Ni, respectively. In addition, weak satellites due to Se–Se coupling ($^2J_{Se-Se} = 138$ Hz) are observed, consistent with the Se_2^{2-} bonding mode and its chemical shift of 608 ppm [23].

NMR spectroscopic studies have also been extended to the selenomolybdate clusters because ^{95}Mo (spin 5/2, natural abundance 15.7%) is an NMR-active nucleus. Actually, the ^{95}Mo NMR technique has been used to identify unknown Mo/Cu/S clusters in solution based on the sensitive probe of the coordination environments of the molybdenum atom [51]. A series of Mo/Cu(Ag, Au)/Se clusters with different structural modes has been examined by ^{95}Mo NMR spectroscopy. The remote deshielding effect on the Mo nucleus from the different coinage-metals in the tetraselenomolybdate system exhibits the trend Au > Cu > Ag [25], which is similar to that in the corresponding tetrathiomolybdate system [52]. However, the deshielding effect of the coinage metal in the tetraselenometalate system is smaller that that in the sulfide system. This may be explained by the larger orbital overlap between Se and Mo than that between S and Mo. A nearly linear correlation with the ^{95}Mo chemical shift was formed for the products of the additional coordination reaction $[MoS_4]^{2-}$ with CuX (X = halide, PPh_3 or S_2CNR_2) [53], however, no regularity of the ^{95}Mo chemical shifts was observed for the products of the reaction of $[MoSe_4]^{2-}$ with CuX [54]. Therefore, it is evident that ^{95}Mo chemical shifts are very sensitive to structural variations in the tetraselenometallic clusters. In addition, ^{95}Mo NMR spectroscopy was used to monitor ligand-substitution and cluster skeleton-transformation reactions processes. The results show that the influence of peripheral ligands on the ^{95}Mo chemical shift may be neglected, and the Mo nucleus in the $MoSe_4Cu_4$ core has an almost saturation deshielding effect [19].

^{31}P NMR spectroscopy is a useful technique to probe the structure of phosphine-containing heteroselenometallic clusters. For $(\mu\text{-}WSe_4)[M(PMe_2Ph)_2]_2$ (M = Cu, Ag and Au), as the size of the coinage-metal increases, the ^{31}P resonance shifts downfield. The deshielding shift from Cu^+ to Au^+ is due to the increased M–Se orbital overlap because of Cu^+, Ag^+ and Au^+ all being d^{10} systems [10]. A similar trend is found for $\{MoCu_3Se_3X\}(PPh_3)_3Se$ (X = Cl, Br and I), i.e. the ^{31}P resonances shift upfield as X changes from Cl^- to I^-, and can also be ascribed to a smooth decrease in orbital overlap between copper and halide [30a]. However, this phenomenon is not observed in the corresponding Ag-containing clusters [30b], possibly because of three long Ag–X bonds. No ^{31}P–^{107}Ag coupling was observed in argentoselenometalates, probably because of phosphorus exchange. Furthermore, the coordination geometry of the coinage-metal in the heteroselenometallic cluster may also be inferred from the ^{31}P chemical shift. For example, the observation of two singlets in the ^{31}P NMR spectrum of $(WSe_4)(AgPPh_3)[Ag(PPh_3)_2]$ indicates the presence of two chemically inequivalent phosphorus atoms, and further implies trigonal and tetrahedral coordination of Ag atoms in this cluster compound [26b].

4. NLO properties

Non-linear optics (NLO) is a study that deals mainly with various new optical effects and novel phenomena arising from the interactions of intense coherent optical radiation with matter. Strong NLO properties include relatively large indexes of NLO absorption and refraction. Both the absorption coefficient and refractive

index can be expressed as $\alpha = \alpha_0 + \alpha_2 I$ and $n = n_0 + n_2 I$, respectively, where α_0 and α_2 are the linear and non-linear absorption coefficient, n_0 and n_2 are the linear and non-linear refractive index, respectively, and I is the irradiance of the laser beam within the sample.

NLO research in the last decade has been largely focused on semiconductors, conjugated polymers, and discrete organic molecules [55]. Recently, the fullerene C_{60} has also attracted much attention [56]. By contrast, inorganic clusters, a very promising group of compounds, have received little attention [57]. This is unfortunate because metal clusters may possess the combined strength of both organic polymers and semiconductors. Unlike the case of semiconductors in which little structural modification can be implemented, both the skeleton and terminal elements of the clusters can be altered and/or removed so that modification of NLO properties can be realized through structural manipulation. Also, the incorporation of heavy atoms introduces more sublevels into the energy hierarchy as compared to organic molecules with the same number of skeletal atoms, and this permits a greater number of allowed electron transitions to take place and hence larger NLO effects. Therefore, the incorporation of heavy atoms into clusters may be especially beneficial to NLO applications if the linear absorption can be kept low. With metal clusters, this can be accomplished via proper choice of constituent elements, structural type and peripheral ligands of the cluster [58].

In the past five years, our efforts on thiometalate $[MO_nS_{4-n}]^{2-}$ (M = Mo or W; $n = 0$–2) derivatives have been largely devoted to preparing heterobimetallic sulfur-containing clusters using the low-heating solid-state reaction method and exploring the structure–property relationships with the NLO properties [8,22]. The clusters studied include linear, butterfly, nest, cubane-like, incomplete-cubane, cross-frame and cage shaped types. We have noticed that structural alterations of the clusters give rise to variations in the NLO properties, and substitution of skeletal atoms induced larger effects. For example, nest-shaped clusters $[NBu^n_4]_2[MoCu_3OS_3BrCl_2]$ and $[NBu^n_4]_2[MoCu_3OS_3(NCS)_3]$ [59], a supercage-shaped cluster $[NBu^n_4]_4[Mo_8Cu_{12}O_8S_{24}]$ [60], a twin nest-shaped cluster $[NEt_4]_4[Mo_2Cu_6O_2S_6Br_2I_4]$ [61], a hexagonal prism-shaped cluster $[W_2Ag_4S_8(PPh_3)_4]$ [62], and linear clusters $[MAu_2S_4(AsPh_3)_2]$ (M = Mo, W) [63] show strong NLO behavior. Butterfly-shaped clusters $[MCu_2OS_3(PPh_3)_n]$ (M = Mo, W; $n = 3$, 4) [64], half-open cage-shaped clusters $[NEt_4]_3[W(CuBr)_3OS_3Br]$ [65] and $[MoCu_3OS_3(PPh_3)_3\{S_2P(OBu^n)_2\}]$ [66] and one-dimensional linear chain polymeric clusters $\{[NBu^n_4][MS_4Tl]\}_n$ (M = Mo, W) [67] exhibit large NLO refraction. Cubane-like clusters $[NBu^n_4]_3[MM'_3S_4BrX_3]$ (M = Mo, W; M′ = Cu, Ag; X = Cl, I) possess strong NLO absorption [68]. A very large optical limiting effect has been observed in a hexagonal prism-shaped cluster $[Mo_2Ag_4S_8(PPh_3)_4]$ [69] and a cross-frame cluster $[WCu_4S_4(SCN)_2(py)_6]$ [70].

Conceptually, the corresponding heteroselenometallic clusters were believed to have better NLO behavior compared with their sulfur analogs. An important reason is that a heavy atom effect, Se rather than S, may result in an effective improvement in NLO properties. Moreover, it is well known that selenium-containing compounds have important applications such as precursors for low-bandgap semiconductors and non-linear optics [71].

4.1. Optical limiting effect and the limiting threshold

An optical limiter must provide protection over a wide range of incident intensity or fluence. Optical limiting (OL) can be achieved by means of various nonlinear optical mechanisms, including self-focusing, self-defocusing, induced scattering, and induced-refraction in nonlinear optical media. In a general case, at some critical intensity or threshold in an ideal limiter, the transmittance changes abruptly and exhibits an intensity or fluence dependence. This critical point is called the threshold of the device, while the clamped output is called the limiting value of intensity or fluence. Thus, the limiting threshold is defined as the incident fluence at which the actual transmittance falls to 50% of the corresponding linear transmittance. A high limiting threshold indicates relatively poor optical limiting ability; on the contrary, a lower threshold indicates a large optical limiting effect.

Fluence, as well as intensity, is a physical parameter concerning optical energy or power. Fluence units are J/m^2 (SI), or erg/cm^2 (egs). Intensity units are W/m^2 (SI), or erg/s-cm^2 (egs).

Self-focusing occurs when a light beam of non-uniform intensity falls on a medium with a nonlinear index of refraction. It has the effect of creating a positive lens that tends to defocus the beam. A positive sign for refraction nonlinearity (n_2) has a self-focusing property, while a negative sign for the refractive nonlinearity gives rise to self-defocusing behaviour.

The pump-probe experiment is a technique to study the nonlinear response. The equipment uses a Q-switched, mode-locked, frequency-doubled Nd:YAG laser at 532 or 1064 nm wavelength. As the pump energy increases, namely, the pulse repetition rate (SI unit in Hz) increases, the sample becomes less effective in optical limiting and a larger threshold value is observed. The optical course in this phenomenon is called the pump-probe response.

The optical limiting (OL) effect of typical cubane-like clusters $[MoSe_4M'_3(PPh_3)_3Cl]$ (M′ = Cu, Ag) was first investigated [29]. The thresholds of two samples under the 0.5 Hz repetition-rate condition at 532 nm are 1.8

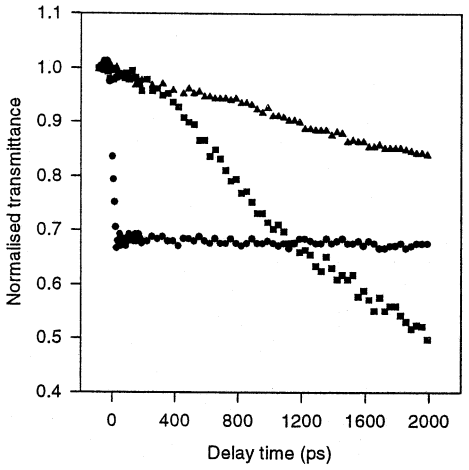

Fig. 15. Normalized transmittance of the probe as a function of time delay for a pump fluence of 1.14 J cm^{-2}: C_{60} in toluene (●), clusters $[MoSe_4M'_3(PPh_3)_3Cl]$ in CH_2Cl_2 for M′ = Cu (▲) and Ag (■). (Reprinted by permission from J. Phys. Chem. 104 (2000) 3448. Copyright 2000 ACS.)

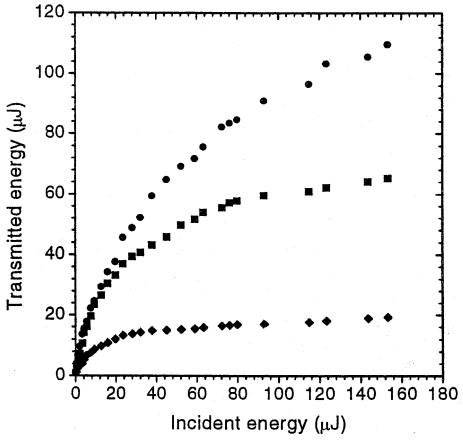

Fig. 16. Optical limiting effects of clusters $[WSe_4\{Cu(dppm)\}_4][ClO_4]_2$ (◆), $[NEt_4]_2[WSe_4(CuS_2CNMe_2)_4]$ (■) and $[NEt_4]_2[WSe_4(CuS_2CNEt_2)_3]$ (●) at 532 nm wavelength with linearly polarized 7 ns pulses.

and 0.8 J cm^{-2} for Cu- and Ag-containing cubane clusters, respectively. To test their effectiveness as broad band optical limiters, 1064 nm wavelength laser pulses from a nanosecond Nd:TAG laser were used. The results show that the limiting threshold of the Ag-containing cluster $[MoSe_4Ag_3(PPh_3)_3Cl]$ is about three times larger at 1064 nm than at 532 nm, while the Cu-containing cluster $[MoSe_4Cu_3(PPh_3)_3Cl]$ does not show an obvious limiting effect. Compared with sulfur-containing clusters, where the optical limiting effect can only be achieved in 15 to 20 s intervals [59–70], the limiting power for $Mo_2Ag_4S_8(PPh_3)_4$ was found to have the best optical limiting effect among analogous sulfur clusters. The value measured at 1064 nm is a factor of ~30 less effective than that at 532 nm [72]. The pump probe experiment was also used further to confirm the non-linear origin of two cubane clusters. Fig. 15 shows the pump probe experimental results of two cluster compounds with a pump fluence of 1.14 J cm^{-2}. Even if the pulse repetition rate increases from 10 to 0.5 Hz, the optical limiting effect of the clusters is still retained, although the limiting threshold values become a little higher. Thus, very good photostability was observed in the optical limiting determinations of two samples, suggesting that nanosecond-response non-linearity is very effective for nanosecond laser pulses. In addition, the pump-probe response of the Cu-containing cluster $[MoSe_4Cu_3(PPh_3)_3Cl]$ in CH_2Cl_2 solution was found to be similar to that of carbon black suspensions (CBS) [73].

Similar to the cross-frame sulfur cluster compound $[WCu_4S_4(SCN)_2(py)_6]$, the analogous selenide cluster $[WSe_4\{Cu(dppm)\}_4][ClO_4]_2$ has a larger optical limiting effect [31]. However, another cross-frame selenide cluster $[NEt_4]_2[WSe_4(CuS_2CNMe_2)_4]$ has a higher limiting threshold [34]. These results may be explained in terms of the electronic effect of the peripheral ligands. Strong σ-donor ligands, such as py, PPh_3 and dppm, move electron density from the Cu-complex fragments toward the $[WE_4]^{2-}$ (E = S and Se) moiety. The π-conjugating ligand $R_2NCS_2^-$ conjugates the Cu(I)-complex and the $[WSe_4]^{2-}$ moiety, resulting in delocalization of electron density among the metal atoms. A relatively poor optical limiting ability was found in the T-frame cluster compound $[NEt_4]_2[WSe_4(CuS_2CNEt_2)_3]$, probably due to a structural difference between cross-frame and T-frame. The optical limiting effects in these coplanar metal atom clusters are depicted in Fig. 16.

Two heterometallic polymeric clusters were initially synthesized to detect their NLO properties. These polymeric clusters show good photostability in optical measurements [20]. The one-dimensional helical chain cluster $\{[La(Me_2SO)_8[(\mu\text{-}WSe_4)_3Ag_3]\}_n$ exhibits both strong optical absorption and optical self-focusing (effective $\alpha_2 = 2.2 \times 10^{-9}$ m W^{-1}, $n_2 = 6.8 \times 10^{-15}$ m^2 W^{-1}; examined in a 0.13 mM DMF solution). The three-dimensional cross-framework cluster $\{[Et_4N]_2[(\mu_4\text{-}WSe_4)Cu_4(CN)_4]\}_n$ shows a larger optical limiting effect (the limiting threshold is ca. 0.2 J cm^{-2}) than the one-dimensional helical chain cluster $\{[La(Me_2SO)_8][(\mu\text{-}WSe_4)_3Ag_3]\}_n$ (the limiting threshold is ca. 0.7 J cm^{-2}). The polymeric selenometallic clusters might be considered to be a very promising candidates for broad-band optical limiting applications, because he optical limiting capability of the three-dimensional cross-framework cluster $\{[Et_4N]_2[(\mu_4\text{-}WSe_4)Cu_4(CN)_4]\}_n$ is better than that of C_{60} [74] and other inorganic clusters [65,66,70] and is comparable to that of phthalocyanine derivatives [75]. Thus, to achieve the desired NLO function, we shall attempt to synthesize new heteroselenometallic clusters with versatile polymeric structural types.

5. Outlook

Although great progress has been made in the last decade, heteroselenometallic cluster chemistry is still an emerging field with many questions remaining to be answered. This diversity can be chiefly attributed to the fact that tetraselenometalates respond easily, by adjusting their coordination mode, to the demands of the metal ions, whether these demands are of an electronic or steric nature. The versatile coordination abilities of tetraselenometalates as well as tetrathiometalates are indicated by the variety of structures exhibited by their heterometallic compounds which can be discrete complexes, clusters and even polymeric networks. Of course, we also need to synthesize specifically predicted and designed structural compounds. On the other hand, synthetic methods such as conventional solution reaction and low-heating solid-state reaction techniques [76], are now emerging as powerful tools in the preparation of these clusters. Although many heteroselenometallic clusters have been synthesized, many aspects of their reaction chemistry remain unexplored, and mechanistic issues have seldom been addressed thus far. Furthermore, the reactivity of tetraselenometalates with organometallic complexes is only poorly explored [77]. Our interest in this area will mainly focus on the exploration of new inorganic clusters with desired NLO properties and the development of new synthetic routes for organometallic clusters with $[MSe_4]^{2-}$ (M = Mo, W) anions. The synthesis and characterization of new types of heteroselenometallic clusters with novel structural modes is expected to continue.

Acknowledgements

We are grateful to the Ministry of Education of China and the Hong Kong University of Science and Technology for support of this research.

References

[1] (a) R.R. Chianelli, Catal. Rev. Sci. Eng. 26 (1984) 361;
(b) F.E. Massoth, G. Muralidhar, in: H.P. Barry, P.C. Mitchell (Eds.), Proceedings of the Climax Fourth International Conference on the Chemistry and Uses of Molydenum, Climax Molybdenum Compary, Ann Arbor, MI, 1982, p. 343.
[2] M.R. Dubois, Chem. Rev. 89 (1989) 1.
[3] (a) D. Coucouvanis, D. Swenson, P. Stremple, C.N. Baenziger, J. Am. Chem. Soc. 101 (1979) 339;
(b) R.H. Holm, J.M. Berg, Acc. Chem. Res. 19 (1986) 363.
[4] E.I. Stiefel, K. Matsumoto (Eds.), Transition Metal Sulfur Chemistry, ACS Symp. Ser. 653, 1996, pp. 216–307, and references cited therein.
[5] A. Müller, E. Diemann, R. Jostes, H. Bögge, Angew. Chem., Int. Ed. Engl. 20 (1981) 934.
[6] (a) S. Sarkar, S.B.S. Mishra, Coord. Chem. Rev. 59 (1984) 239;
(b) A. Müller, E. Diemann, Adv. Inorg. Chem. 31 (1987) 89.
[7] C.E. Hollway, M. Melnik, Rev. Inorg. Chem. 13 (1993) 233.
[8] H.W. Hou, X.Q. Xin, S. Shi, Coord. Chem. Rev. 153 (1996) 25.
[9] (a) M.A. Ansari, J.A. Ibers, Coord. Chem. Rev. 100 (1990) 233;
(b) J.W. Kolis, Coord. Chem. Rev. 105 (1990) 195.
[10] C.C. Christuk, M.A. Ansari, J.A. Ibers, Inorg. Chem. 31 (1992) 4365.
[11] S.C. O'Neal, J.W. Kolis, J. Am. Chem. Soc. 110 (1988) 1971.
[12] A. Müller, U. Wienböker, M. Penk, Chimia 43 (1989) 50.
[13] C.C. Christuk, J.A. Ibers, Inorg. Chem. 32 (1993) 5105.
[14] R.J. Salm, J.A. Ibers, Inorg. Chem. 33 (1994) 4216.
[15] M.A. Ansari, J.C. Bollinger, C.C. Christuk, J.A. Ibers, Acta Crystallogr., Sect C 50 (1994) 869.
[16] R.J. Salm, A. Misetic, J.A. Ibers, Inorg. Chim. Acta 240 (1995) 239.
[17] L.C. Roof, J.W. Kolis, Chem. Rev. 93 (1993) 1037.
[18] Q.F. Zhang, R. Cao, M.C. Hong, H.Q. Liu, J.X. Lu, Chin. J. Struct. Chem. 17 (1998) 112.
[19] M.C. Hong, Q.F. Zhang, R. Cao, D.X. Wu, J.T. Chen, W.J. Zhang, H.Q. Liu, J.X. Lu, Inorg. Chem. 36 (1997) 6251.
[20] Q.F. Zhang, W.H. Leung, X.Q. Xin, H.K. Fun, Inorg. Chem. 39 (2000) 417.
[21] (a) W.S. Chen, J.M. Stewart, R.A. Mickelsen, Appl. Phys. Lett. 46 (1985) 1095;
(b) K.-W. Kim, M.G. Kanatzidis, J. Am. Chem. Soc. 114 (1992) 4979;
(c) I. Dance, G. Lee, Spec. Publ., R. Soc. Chem. (1993) 131;
(d) H.B. Singh, N. Sudha, Polyhedron 15 (1996) 745.
[22] (a) S. Shi, W. Ji, S.H. Tang, J.P. Lang, X.Q. Xin, J. Am. Chem. Soc. 116 (1994) 3615;
(b) H.W. Hou, X.R. Ye, X.Q. Xin, J. Liu, M.Q. Chen, S. Shi, Chem. Mater. 7 (1995) 472;
(c) H.W. Hou, D.L. Long, X.Q. Xin, X.Y. Huang, B.S. Kang, P. Ge, W. Ji, S. Shi, Inorg. Chem. 35 (1996) 5363;
(d) P. Ge, S.H. Tang, W. Ji, S. Shi, H.W. Hou, D.L. Long, X.Q. Xin, S.F. Lu, Q.J. Wu, J. Phys. Chem. B 101 (1997) 27.
[23] M.A. Ansari, C.-N. Chau, C.H. Mahler, J.A. Ibers, Inorg. Chem. 28 (1989) 650.
[24] A. Müller, H. Bögge, U. Schimanski, M. Penk, K. Nieradzik, D. Dartmann, E. Krickemyer, J. Schimanski, C. Römer, M. Römer, H. Dornfeld, U. Wienböker, W. Hellmann, M. Zimmermann, Monatsch. Chem. 120 (1989) 367.
[25] Q.F. Zhang, R. Cao, M.C. Hong, D.X. Wu, W.J. Zhang, Y. Zheng, H.Q. Liu, Inorg. Chim. Acta 271 (1998) 93.
[26] (a) A. Müller, U. Schimanski, J. Schimanski, Inorg. Chim. Acta L 76 (1983) 245;
(b) Q.F. Zhang, W.H. Leung, Y.L. Song, M.C. Hong, X.Q. Xin, New. J. Chem. 25 (2001) 465.
[27] Q.M. Wang, X.T. Wu, Q. Huang, T.L. Sheng, P. Lin, Polyhedron 16 (1997) 1439.
[28] S.W. Du, X.T. Wu, J.X. Lu, Polyhedron 12 (1994) 841.
[29] Q.F. Zhang, Y.N. Xiong, T.S. Lai, W. Ji, X.Q. Xin, J. Phys. Chem. B 104 (2000) 3476.
[30] (a) Q.F. Zhang, M.C. Hong, W.P. Su, R. Cao, H.Q. Liu, Polyhedron 16 (1997) 1433;
(b) Q.F. Zhang, M.C. Hong, H.Q. Liu, Transition Met. Chem. 22 (1997) 156;
(c) Q.F. Zhang, X.Q. Xin, M.C. Hong, R. Cao, S.S.S. Raj, H.-K. Fun, Acta Crystallogr., Sect. C 55 (1999) 726.
[31] C.C. Christuk, M.A. Ansari, J.A. Ibers, Angew. Chem., Int. Ed. Engl. 31 (1992) 1477.
[32] Q.F. Zhang, M.C. Hong, R. Cao, H.Q. Liu, Chin. J. Inorg. Chem. 13 (1997) 179.
[33] M.C. Hong, M.H. Wu, X.Y. Huang, F.L. Jiang, R. Cao, H.Q. Liu, J.X. Lu, Inorg. Chim. Acta 260 (1997) 73.

[34] Q.F. Zhang, M.T. Bao, M.C. Hong, R. Cao, Y.L. Song, X.Q. Xin, J. Chem. Soc., Dalton Trans. (2000) 605.
[35] D. Coucouvanis, Prog. Inorg. Chem. 26 (1979) 301.
[36] R. Cao, Q.F. Zhang, W.P. Su, M.T. Bao, M.C. Hong, Polyhedron 18 (1999) 333.
[37] Q.F. Zhang, S.S.S. Raj, H.-K. Fun, X.Q. Xin, Chem. Lett. (1999) 619.
[38] C.K. Chan, C.X. Guo, R.J. Wang, T.C.M. Mak, C.M. Che, J. Chem. Soc., Dalton Trans. (1995) 735.
[39] (a) A. Müller, Polyhedron 5 (1986) 323;
(b) K.P. Callahan, P.A. Piliero, Inorg. Chem. 19 (1980) 2619.
[40] Q.F. Zhang, S.S.S. Raj, M.C. Hong, R. Cao, H.K. Fun, X.Q. Xin, Inorg. Chem. Commun. 2 (1999) 272.
[41] P. Braunstein, J. Kervennal, J.-L. Richert, Angew. Chem., Int. Ed. Engl. 24 (1985) 768.
[42] M.A. Greaney, C.L. Coyle, R.S. Pilato, E.I. Stiefel, Inorg. Chim. Acta 189 (1991) 81.
[43] R.H. Holm, Adv. Inorg. Chem. 38 (1992) 1.
[44] Q.F. Zhang, R. Cao, M.C. Hong, H.Q. Liu, J.X. Lu, Sci. China B 42 (2000) 75.
[45] Y.-J. Lu, J.A. Ibers, Acta Crystallogr., Sect. C 47 (1991) 1600.
[46] (a) A. Müller, M. Dartmann, C. Römer, W. Clegg, G.M. Sheldrick, Angew. Chem., Int. Ed. Engl. 20 (1981) 1060;
(b) J.P. Lang, J. Liu, M.Q. Chen, J.M. Lu, G.Q. Bian, X.Q. Xin, J. Chem. Soc., Chem. Commun. (1994) 2665;
(c) Q. Huang, X.T. Wu, Q.M. Wang, T.L. Sheng, J.X. Lu, Angew. Chem., Int. Ed. Engl. 35 (1996) 868.
[47] Q.F. Zhang, C. Zhang, Y.L. Song, X.Q. Xin, J. Mol. Struct. 525 (2000) 79.
[48] A.B.P. Lever, Inorganic Electronic Spectroscopy, Elsevier, New York, 2nd edn., 1984, Chapter 5.
[49] Q.F. Zhang, Master's Thesis, Chinese Academy of Sciences, 1997.
[50] (a) R.W.M. Wardle, C.H. Mahler, C.-N. Chau, J.A. Ibers, Inorg. Chem. 27 (1988) 2790;
(b) M.A. Ansari, C.H. Mahler, G.S. Chorghade, Y.-J. Lu, J.A. Ibers, Inorg. Chem. 29 (1990) 3832.
[51] M. Minelli, J.H. Enemark, Coord. Chem. Rev. 68 (1985) 169.
[52] J.M. Charnock, S. Bristow, J.R. Nicholson, C.D. Garner, J. Chem. Soc., Dalton Trans. (1987) 303.
[53] M. Minelli, J.H. Enemark, J.R. Nicholson, C.D. Garner, Inorg. Chem. 23 (1984) 4384.
[54] Q.F. Zhang, R. Cao, D.X. Wu, M.C. Hong, H.Q. Liu, Chin. J. Magn. Reson. 15 (1998) 9.
[55] (a) S.R. Marder, J.E. Sohn, G.D. Stucky (Eds.), Materials for Nonlinear Optics, Chemical Perspectives, American Chemical Society, Washingdon, DC, 1991;
(b) H.S. Nalwa, S. Miyata (Eds.), Nonlinear Optics of Organic Moleculaes and Polymers, CRC Press, Boca Raton, FL, 1997.
[56] (a) L.W. Tutt, A. Kost, Nature 19 (1992) 225;
(b) T.H. Wei, D.J. Hagan, M.J. Sence, E.W. Van Stryland, J.W. Perryand, D.R. Coulter, Appl. Phys. B 54 (1992) 46.
[57] G.R. Allan, D.R. Labergerie, S.J. Rychnovsky, T.F. Boggess, A.L. Smirl, J. Phys. Chem. 96 (1992) 6313.
[58] S. Shi, Z. Lin, Y. Mo, X.Q. Xin, J. Phys. Chem. 100 (1996) 10696.
[59] S. Shi, W. Ji, W. Xie, T.C. Chong, H.C. Zeng, J.P. Lang, X.Q. Xin, Mater. Chem. Phys. 39 (1995) 298.
[60] S. Shi, W. Ji, X.Q. Xin, J. Phys. Chem. 99 (1995) 894.
[61] H.W. Hou, X.Q. Xin, J. Liu, M.Q. Chen, S. Shi, J. Chem. Soc., Dalton Trans. (1994) 3211.
[62] G. Sankane, T. Shibahara, H.W. Hou, X.Q. Xin, S. Shi, Inorg. Chem. 34 (1995) 4785.
[63] H.G. Zheng, W. Ji, M.L.K. Low, G. Sakane, T. Shibahara, X.Q. Xin, J. Chem. Soc., Dalton Trans. (1997) 2357.
[64] S. Shi, H.W. Hou, X.Q. Xin, J. Phys. Chem. 99 (1995) 4050.
[65] Z.R. Chen, H.W. Hou, X.Q. Xin, K.B. Yu, S. Shi, J. Phys. Chem. 99 (1995) 8717.
[66] D.L. Long, S. Shi, X.Q. Xin, B.S. Luo, L.R. Chen, X.Y. Huang, B.S. Kang, J. Chem. Soc., Dalton Trans. (1996) 2617.
[67] J.P. Lang, K. Tatsumi, H. Kawaguchi, J.M. Lu, P. Ge, W. Ji, S. Shi, Inorg. Chem. 35 (1996) 7924.
[68] (a) S. Shi, W. Ji, J.P. Lang, X.Q. Xin, J. Phys. Chem. 98 (1994) 3570;
(b) W. Ji, H.J. Du, S.H. Tang, S. Shi, J. Opt. Soc. Am. B 12 (1996) 876.
[69] W. Ji, S. Shi, H.J. Du, P. Ge, S.H. Tang, X.Q. Xin, J. Phys. Chem. 99 (1995) 17297.
[70] M.K.M. Low, H.W. Hou, H.G. Zheng, W.T Wong, G.X. Jin, X.Q. Xin, W. Ji, Chem. Commun. (1998) 505.
[71] See any issue of The Bulletin of the Selenium–Tellurium Development Association, Grimbergen, Belgium.
[72] T. Xia, A. Dogariu, K. Mansour, D.J. Hagan, A.A. Said, E.W. Van Stryland, S. Shi, J. Opt. Soc. Am. B 15 (1998) 1497.
[73] Y.N. Xiong, Q.F. Zhang, W.L. Tan, X.Q. Xin, W. Ji, Appl. Phys. A 70 (2000) 85.
[74] D.G. McLean, R.L. Sutherland, M.C. Brant, D.M. Brandelik, P.A. Fleitz, T. Pottenger, Opt. Lett. 18 (1993) 858.
[75] J.W. Perry, K. Mansour, S.R. Marder, K.J. Perry Jr., D. Alvarez, I. Choong, Opt. Lett. 19 (1994) 625.
[76] (a) J.P. Lang, X.Q. Xin, J. Solid State Chem. 108 (1994) 118;
(b) J.P. Lang, K. Tatsumi, Inorg. Chem. 37 (1998) 6308.
[77] K.E. Howard, T.B. Rauchfuss, S.R. Wilson, Inorg. Chem. 27 (1988) 1710.